Geol. Mag. **154** (*6*), *2017, pp. 1360–1370. © Cambridge University Press 2016*
doi:10.1017/S0016756816001138

Evidence for marine redox control on spatial colonization of early animals during Cambrian Age 3 (*c.* 521–514 Ma) in South China

CHENGSHENG JIN*, CHAO LI*†, THOMAS J. ALGEO*‡§, MENG CHENG*, LIDAN LEI*, ZIHU ZHANG* & WEI SHI*

*State Key Laboratory of Biogeology and Environmental Geology, China University of Geosciences, Wuhan 430074, China
‡State Key Laboratory of Geological Processes and Mineral Resources, China University of Geosciences, Wuhan 430074, China
§Department of Geology, University of Cincinnati, Cincinnati, OH 45221-0013, USA

(*Received* 28 July 2016; *accepted* 8 November 2016; *first published online* 29 December 2016)

Abstract – The early Cambrian Period was a key interval in Earth history with regard to changes in both ocean chemistry and animal evolution. Although increasing ocean ventilation has been widely assumed to have played a key role in the rapid appearance, diversification and spatial colonization of early animals, this relationship is in fact not firmly established. Here, we report a high-resolution Fe-C-S-Al-Ti geochemical study of the lower Cambrian Wangjiaping section from an outer-shelf setting of the Yangtze Sea of South China. Iron speciation data document a redox transition from dominantly euxinic to ferruginous conditions during Cambrian Age 3 (*c.* 521–514 Ma). Interpretation of coexisting pyrite sulphur isotope ($\delta^{34}S_{py}$) records from Wangjiaping reveals relatively high marine sulphate availability at Wangjiaping. Furthermore, Wangjiaping section shows lower $\delta^{34}S_{py}$ (–2.1 ± 5.3 ‰) and lower TOC (2.4 ± 1.1 %) values but higher positive correlation ($R^2 = 0.66$, $p < 0.01$) between TOC and Fe_{py}/Fe_{HR} relative to deeper sections reported previously, suggesting that euxinia developed at Wangjiaping in response to increasing marine productivity and organic matter-sinking fluxes. Our reconstructed redox conditions and fossils at Wangjiaping in comparison with previously well-studied strata in the inner-shelf Xiaotan and Shatan sections suggest that planktonic and benthic planktonic trilobites with bioturbation appeared in the oxic water columns, whereas only planktonic trilobites without bioturbation occurred within the anoxic (even euxinic) water columns during Cambrian Age 3. This finding indicates that spatial heterogeneity of redox conditions in the shelves had an important effect on early animal distribution in the Yangtze Block.

Keywords: early Cambrian, early animal, South China, redox, euxinia

1. Introduction

The early Cambrian Period witnessed a profound shift from a marine ecosystem dominated by cyanobacteria to one similar to a modern-day ecosystem represented by eukaryotic algae and animals (Butterfield, 2007, 2011). This biotic event, which was also characterized by the rapid emergence and diversification of complex skeletal animals, was known as the 'Cambrian Explosion' (Steiner *et al*. 2007; Zhu, 2010; Shu *et al.* 2014). Strata of this age exhibit a pronounced spatial heterogeneity in the distribution of body fossils and bioturbation (Zhu, 2010; Buatois *et al*. 2016). For example, during Cambrian Age 3 (*c.* 521–514 Ma), shallow-water sections such as Xiaotan (Yunnan) yield abundant planktonic and benthic trilobites and intensive bioturbation, whereas deeper-water sections such as Wangjiaping (Hubei) yield few benthic but abundant planktonic trilobites without evidence of bioturbation (Zhu, 2010).

Animal evolution during early Cambrian time is widely inferred to have been linked to rising oxygen levels in the atmospheric–oceanic system (Nursall, 1959; Knoll & Carroll, 1999; Sperling *et al*. 2013). Evidence in support of this inference includes increases in marine sediment Mo and U concentrations and in $\delta^{98/95}$Mo values (to +2.34 ‰, which is close to modern values), suggesting seawater oxygen concentrations close to those of the modern ocean (Chen *et al*. 2015*b*). This nearly full oceanic oxygenation coincided with the appearance of nearly all metazoan body plans and a rise of metazoan body size represented by the Chengjiang Biota of Cambrian Age 3. However, other studies making use of geochemical redox proxies have inferred that early Cambrian deep-water settings remained anoxic and ferruginous (e.g. Canfield *et al*. 2008; Sperling *et al*. 2015) or even euxinic (e.g. Goldberg *et al*. 2007; Wille *et al*. 2008). Recent geochemical investigations have documented highly heterogeneous redox conditions for the Yangtze Sea during early Cambrian time, in which mid-depth euxinic waters existed dynamically between oxic surface waters and ferruginous deep waters (Feng *et al*. 2014; Jin *et al*. 2016; Och *et al*. 2016). This pattern, dubbed the 'euxinic wedge model' (Li *et al*. 2010, 2015*a*; Li, Zhu & Chu, 2016), may provide new insights regarding the

†Author for correspondence: chaoli@cug.edu.cn

influence of spatially heterogeneous redox conditions on early animal evolution.

In order to investigate the relationship between redox heterogeneity and early animal evolution, we conducted a high-resolution Fe-S-C-Al-Ti chemostratigraphic study of the outer-shelf Wangjiaping section from lower Cambrian strata of the Yangtze Block. The record of animal evolution at Wangjiaping is different from that at typical inner-shelf sections, such as Xiaotan (Yunnan Province) and Shatan (Sichuan Province). At Wangjiaping, the Shuijingtuo Formation yielded a few benthic trilobites of *Metaredlichia* sp. belonging to the Redlichiacea but abundant planktonic trilobites represented by Eodiscina, which are different from the abundant planktonic and benthic trilobites belonging to the Redlichiacea from the correlative strata at Xiaotan and Shatan (Xiang *et al*. 1987). Our new data, in combination with published Fe-speciation data from the inner-shelf Xiaotan and Shatan sections, provided us with an opportunity to evaluate the relationship between redox heterogeneity and animal spatial distribution on the early Cambrian Yangtze Block.

2. Materials and methods

A total of 34 samples were collected from fresh outcrop at Wangjiaping in July 2015. Large rock blocks (>200 g) were sampled and all potentially weathered surfaces, post-depositional veins, and visible pyrite nodule and bands were trimmed away prior to powdering. Each sample was crushed into powders for measurement of total organic (TOC) and carbonate (TIC) carbon, iron speciation data, Al, Ti and pyrite sulphur isotopic compositions ($\delta^{34}S_{py}$). All geochemical data were generated at the State Key Laboratory of Biogeology and Environmental Geology, China University of Geosciences (Wuhan).

TIC was determined by the difference between total carbon (TC) and TOC, measured using a Jena Multi-EA 4000 carbon-sulphur analyser. For TC analysis, *c.* 100 mg of powder were weighed into a ceramic boat, combusted at 1350 °C and measured using calibrated infrared sensors. For TOC analysis, *c.* 500 mg of powder were treated with 4-N HCl to remove carbonate, washed several times with deionized water to remove HCl residue, and finally dried overnight at 50 °C. About 100 mg of the residue were analysed for TOC content following the same procedures as for TC. Analytical uncertainty is better than ±0.2 % for TC and TOC based on replicate analyses of Alpha Resources standard AR-4007 (TC = 7.62 %).

Highly reactive iron (Fe_{HR}) is the sum of carbonate-associated Fe (Fe_{carb}), Fe oxides (Fe_{ox}), magnetite Fe (Fe_{mag}) and pyrite Fe (Fe_{py}) (i.e. $Fe_{HR} = Fe_{carb} + Fe_{ox} + Fe_{mag} + Fe_{py}$). Fe sequential extractions were conducted following standard procedures for Fe_{carb}, Fe_{ox} and Fe_{mag} (Poulton & Canfield, 2005). About 100 mg of sample powder was treated with a sodium acetate solution buffered to a pH of 4.5 by addition of analytical-grade acetic acid at 50 °C for 48 h to extract Fe_{carb}. The sample residue from the first step was treated with a 50 g L^{-1} sodium dithionite solution buffered to a pH of 4.8 by addition of 0.2 M sodium citrate and analytical-grade acetic acid at room temperature for 2 h to extract Fe_{ox}. The sample residue from the second step was treated with a 0.2 M ammonium oxalate and 0.17 M oxalic acid solution buffered to a pH of 3.2 by addition of analytical-grade ammonium water at room temperature for 6 h to extract Fe_{mag}. After dilution with 2 % HNO_3 all extracts were measured for Fe content using atomic absorption spectroscopy (AAS), yielding an RSD of <5 %. Fe_{py} was stoichiometrically determined from chromium reducible pyrite (Canfield *et al*. 1986). Unreactive iron (Fe_U) was determined from the difference between total iron (Fe_T) and Fe_{HR}. A more detailed description of the Fe speciation methods can be found in Li *et al*. (2015*b*).

Fe_T, Al and Ti were determined by X-ray fluorescence spectrometry (XRF) of fused glass beads. About 0.6 g of sample powders, a 6 g mixture of $Li_2B_4O_7$, $LiBO_2$ and LiF, and 0.3–0.4 g of ammonium nitrate as a fluxing medium were loaded into a porcelain crucible and mixed well with a spatula. The mixture was loaded into a platinum crucible, to which was added 5–6 drops of lithium bromide solution, before being finally transferred to the fusion machine to produce a glass bead. Analytical errors are better than ±5 % for Fe_T, Al and Ti based on replicate analyses of two Chinese (GBW07107, GBW07108) standards.

3. Geological background

Palaeogeographic reconstructions show that South China was an isolated, peri-equatorial continental block close to northeastern Gondwana (modern Australia) during early Cambrian time (Fig. 1a; Yang, Steiner & Keupp, 2015; Zhang *et al*. 2015). The South China Block was composed of the Yangtze and Cathaysia blocks, which had been sutured together during the early Neoproterozoic Era, but continued to undergo some compressional deformation as late as the Late Ordovician 'Caledonian' Orogeny (Wang & Li, 2003). During the Ediacaran–Cambrian transition, the Yangtze Block consisted of the shallowly submerged Yangtze Platform bordered on the SE by a ramp descending into the deep-water Nanhua Basin, which had developed over a Neoproterozoic failed rift initialized at *c.* 820 Ma (Wang & Li, 2003).

During the Cambrian Fortunian Age to early Age 2 (*c.* 541–529 Ma), sedimentation on the Yangtze Block was characterized by mainly carbonate deposits on the platform to the NW, interbedded shale, chert and carbonate deposits on the ramp, and mudstone/shale or chert deposits in the basin to the SE (Fig. 1b; Steiner *et al*. 2007; Zhu, Zhang & Yang, 2007). A major transgression since the middle Cambrian Age 2 caused widespread deposition of black shale across the Yangtze Platform.

https://doi.org/10.1017/S0016756816001138 Published online by Cambridge University Press

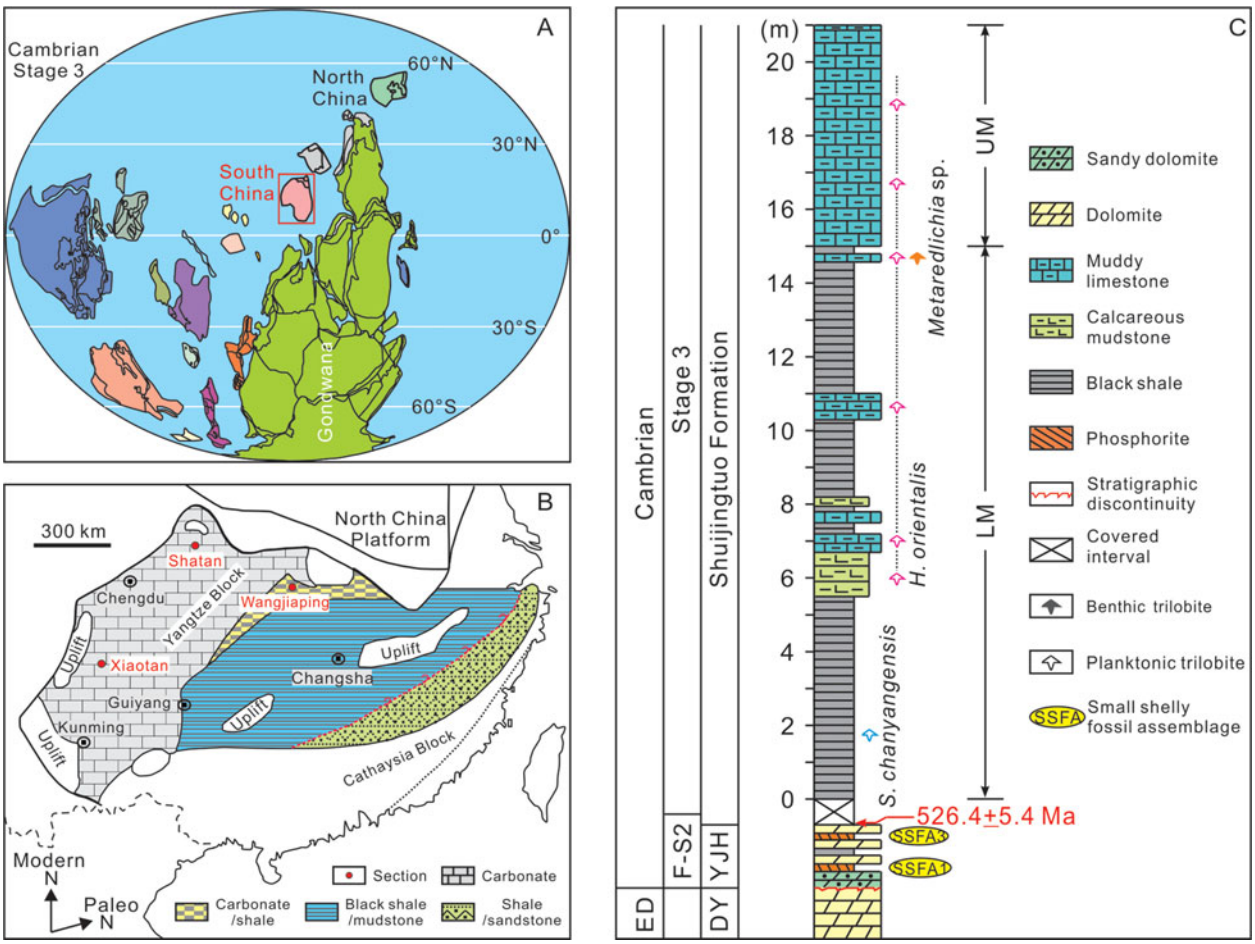

Figure 1. (Colour online) Geological background of study section. (a) Global palaeogeographic reconstruction for Cambrian Stage 3 (modified from Yang, Steiner & Keupp, 2015). (b) Palaeogeography of Yangtze Block during early Cambrian Fortunian and early Stage 2 ages (modified from Goldberg *et al*. 2007). The study section Wangjiaping and two correlated inner-shelf sections Xiaotan and Shatan are marked. (c) Lithological and stratigraphic profiles of the lower Cambrian Wangjiaping section. The U–Pb age is from the nearby Wuhe section (Okada *et al*. 2014). ED – Ediacaran; F – Fortunian Stage; S2 – Stage 2; DY – Dengying Formation; YJH – Yanjiahe Formation; LM – Lower Member; and UM – Upper Member.

The Wangjiaping section (30° 48′ 41″ N and 111° 11′ 12″ E) is sited west of Yichang city in central Hubei Province. Palaeogeographically, this area represented outer-shelf facies during the early Cambrian Period (Zhu *et al*. 2003). The section consists of the Yanjiahe and Shuijingtuo formations (Fig. 1c). The Yanjiahe Formation, which disconformably overlies the late Ediacaran Dengying Formation, consists of sandy dolomite, phosphorite layers, black shale and dolomite. The small shelly fossil assemblages 1 (SSFA1, *Anabarites trisulcantus–Protohertzina unguliformis*) and 3 (SSFA3, *Watsonella crosbyi*) have been identified in the correlative Yanjiahe section, *c.* 15 km to the SW (Chen, 1984). The overlying Shuijingtuo Formation is divided into two members based on lithology: (1) a lower member (LM; 0–15 m) consisting of black shale interbedded with calcareous mudstone and muddy limestone, in which are found abundant planktonic trilobites such as *S. chanyangensis* and *H. orientalis*; and (2) an upper member (UM; 15–21 m) consisting of muddy limestone, in which are found planktonic trilobites such as *H. orientalis* (Xiang *et al*. 1987). Only one benthic trilobite fossil of *Metaredlichia* sp. was found in the muddy limestone layer at *c.* 14.8 m close to the LM–UM boundary (Fig. 1c; Xiang *et al*. 1987). The lithological change from LM to UM is consistent with the marine regression recorded basinwide (Yang, Zhu & Zhang, 2005). A U–Pb zircon age from ash beds at the base of the Shuijingtuo Formation black shale in the Wuhe section located *c.* 30 km to the SW of Wangjiaping provides a maximum age of 526.4 ± 5.4 Ma (i.e. mainly of Age 3) for the Shuijingtuo Formation (Okada *et al*. 2014).

4. Results

The Fe-S-C-Al-Ti data for the Wangjiaping section are provided in Table 1 and Figures 2–4. TOC concentrations range over 0.1–3.6 % (mean 2.0 %) and exhibit a stepwise decreasing trend upsection (Fig. 2). TIC concentrations are relatively variable, ranging over 0.8–11.6 ‰ (mean 4.3 %). $\delta^{34}S_{py}$ ranges from –14.1 to +19.3 ‰ (mean –0.1 ‰). Al ranges over 1.1–10.0 % (mean 6.4 %), roughly increasing upsection in the LM (0–15 m) of the Shuijingtuo Formation; it ranges over 0.7–4.1 % (mean 2.2 %), decreasing upsection in the

https://doi.org/10.1017/S0016756816001138 Published online by Cambridge University Press

Table 1. Key geochemical data in the outer-shelf Wangjiaping section

Lithology[a]	Sample	Height (m)	TOC (wt %)	TIC (wt %)	$\delta^{34}S_{py}$ (‰ VCDT)	Al (wt %)	Ti (wt %)	Fe_{carb} (wt %)	Fe_{ox} (wt %)	Fe_{mag} (wt %)	Fe_{py} (wt %)	Fe_{HR} (wt %)	Fe_T (wt %)	Fe_U[b] (wt %)	Fe_{HR}/Fe_T[c]	Fe_{py}/Fe_{HR}
ML	SHT-34	20.7	0.8	8.5	2.0	3.02	0.14	0.27	0.64	0.05	0.24	1.20	1.43	0.23	0.84	0.20
ML	SHT-33	19.7	0.3	11.0	19.2	1.14	0.05	0.11	0.26	0.00	0.01	0.38	0.45	0.07	0.84	0.03
ML	SHT-32	18.7	0.2	11.6	19.3	0.72	0.03	0.08	0.00	0.00	0.22	0.30	0.32	0.02	0.93	0.73
ML	SHT-31	15.7	0.1	10.1	8.4	1.94	0.09	0.27	0.06	0.05	0.43	0.81	1.03	0.22	0.79	0.53
ML	SHT-30	15.3	0.5	7.2	–4.8	4.14	0.19	0.20	0.12	0.03	0.74	1.09	1.80	0.71	0.60	0.68
ML	SHT-29	15.1	0.1	9.4	9.1	2.40	0.11	0.30	0.05	0.03	0.61	0.99	1.51	0.52	0.66	0.62
BS	SHT-28	12.4	0.1	0.9	–1.0	10.03	0.52	0.34	0.11	0.08	2.25	2.78	5.18	2.40	0.54	0.81
BS	SHT-27	11.8	1.3	0.5	–14.1	9.67	0.53	0.12	0.07	0.06	1.65	1.90	4.08	2.18	0.47	0.87
BS	SHT-26	11.1	1.2	2.0	–11.4	9.12	0.42	0.31	0.10	0.06	1.78	2.25	4.01	1.76	0.56	0.79
ML	SHT-25	11.0	0.1	11.5	6.0	1.09	0.05	0.10	0.01	0.01	1.34	1.46	1.27	0.00	1.00	0.92
ML	SHT-24	10.5	0.8	6.6	–4.5	4.86	0.23	0.48	0.09	0.04	0.92	1.53	2.27	0.74	0.68	0.60
BS	SHT-23	9.5	1.8	1.1	–9.4	9.23	0.45	0.34	0.06	0.06	1.46	1.92	3.99	2.07	0.48	0.76
BS	SHT-22	8.9	1.5	1.9	–9.2	8.85	0.39	0.44	0.15	0.06	1.82	2.47	3.92	1.45	0.63	0.74
BS	SHT-21	8.4	1.3	1.8	–10.3	9.10	0.46	0.47	0.09	0.04	1.83	2.43	4.30	1.87	0.56	0.75
CM	SHT-20	8.0	1.9	4.2	2.7	6.18	0.32	0.30	0.07	0.02	3.4	3.79	4.29	0.50	0.88	0.90
BS	SHT-19	7.9	2.4	1.4	1.1	8.22	0.41	0.21	0.08	0.03	2.91	3.23	4.28	1.05	0.75	0.90
ML	SHT-18	7.7	1.5	8.7	–4.0	2.75	0.14	0.52	0.06	0.00	1.24	1.82	1.78	0.00	1.00	0.68
BS	SHT-17	7.3	2.9	2.9	–0.6	7.16	0.39	0.46	0.05	0.00	4.44	4.95	3.76	0.00	1.00	0.90
ML	SHT-16	7.0	1.5	8.2	0.5	3.33	0.16	0.37	0.06	0.00	1.88	2.31	2.15	0.00	1.00	0.81
CM	SHT-15	6.5	2.8	4.9	1.1	5.21	0.28	0.42	0.05	0.00	2.28	2.75	2.97	0.22	0.93	0.83
CM	SHT-14	6.1	2.3	5.9	3.5	5.17	0.26	0.54	0.07	0.01	2.38	3.00	3.15	0.15	0.95	0.79
CM	SHT-13	5.8	3.0	5.5	0.4	5.66	0.29	0.70	0.15	0.03	2.55	3.43	3.69	0.26	0.93	0.74
BS	SHT-12	5.3	3.2	1.4	–10.7	7.27	0.38	0.25	0.05	0.01	3.14	3.45	3.82	0.37	0.90	0.91
BS	SHT-11	4.6	3.3	1.5	0.0	6.75	0.35	0.29	0.07	0.01	3.87	4.24	4.45	0.21	0.95	0.91
BS	SHT-10	4.3	3.1	1.5	–3.9	6.23	0.36	0.28	0.04	0.00	2.91	3.23	3.61	0.38	0.89	0.90
BS	SHT-9	4.0	3.3	0.8	1.3	6.66	0.38	0.20	0.04	0.00	2.98	3.22	3.68	0.46	0.88	0.93
BS	SHT-8	3.6	3.5	1.6	–2.8	6.24	0.35	0.22	0.04	0.00	2.76	3.02	3.28	0.26	0.92	0.91
BS	SHT-7	3.1	3.2	1.7	–1.3	6.31	0.35	0.21	0.05	0.00	2.36	2.62	3.05	0.43	0.86	0.90
BS	SHT-6	2.8	2.9	2.0	3.9	5.72	0.33	0.29	0.05	0.00	2.25	2.59	2.87	0.28	0.90	0.87
BS	SHT-5	2.5	3.7	2.7	–0.5	5.31	0.29	0.25	0.05	0.00	1.56	1.86	2.84	0.98	0.66	0.84
BS	SHT-4	2.0	3.5	1.9	3.2	5.08	0.28	0.29	0.04	0.00	2.39	2.72	2.91	0.19	0.93	0.88
BS	SHT-3	1.9	3.6	2.5	1.5	5.38	0.28	0.27	0.06	0.00	2.25	2.58	2.90	0.32	0.89	0.87
BS	SHT-2	1.3	3.5	1.6	–2.4	6.86	0.36	0.23	0.12	0.01	2.85	3.21	3.55	0.34	0.91	0.89
BS	SHT-1	0.6	3.2	2.0	2.3	5.22	0.26	0.45	0.04	0.00	2.36	2.85	3.07	0.22	0.93	0.83

[a]BS – black shale; CM – calcareous mudstone; ML – muddy limestone; [b]For samples with measured $Fe_U < 0$, these values are reported as 0; [c] For samples with measured $Fe_{HR}/Fe_T > 1$, these values are reported as 1

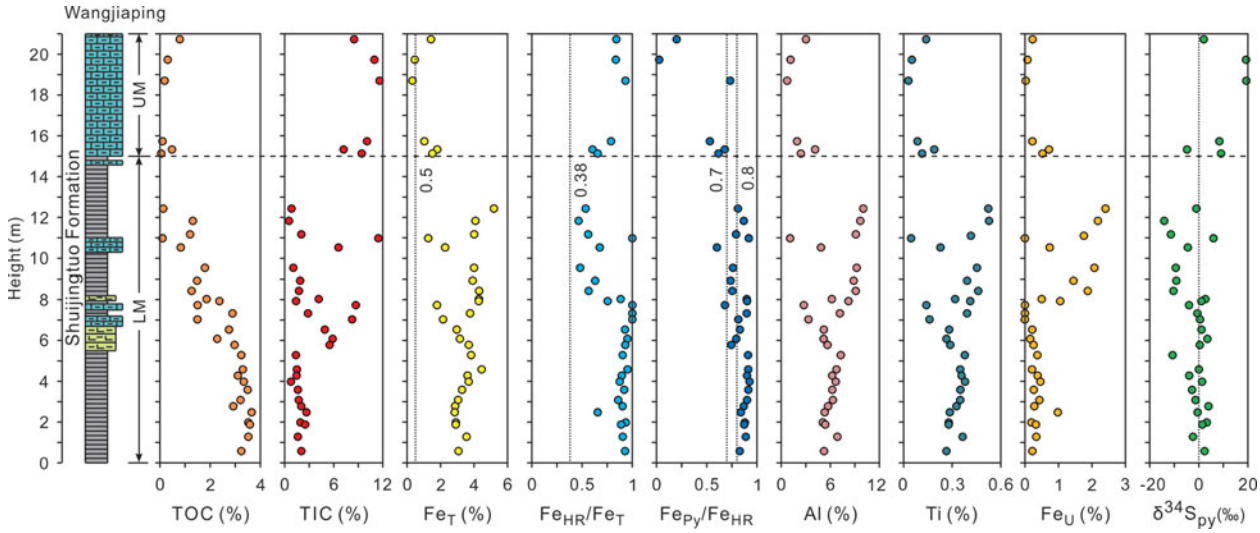

Figure 2. (Colour online) Composite chemostratigraphy of Wangjiaping section. The vertical dashed lines (from left to right) for each section indicate key values of Fe_T (0.5 wt %), Fe_{HR}/Fe_T (0.38) and Fe_{py}/Fe_{HR} (0.7–0.8) used in redox interpretations (see text for details).

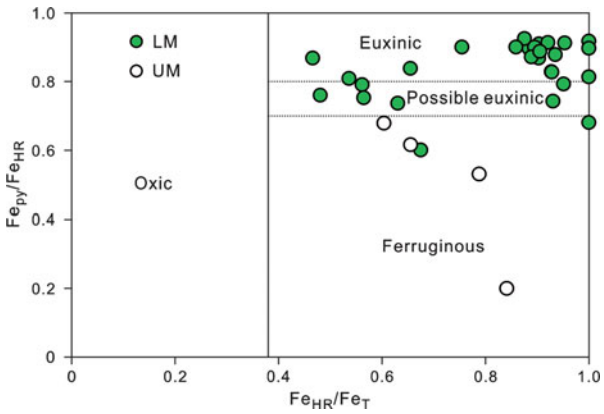

Figure 3. (Colour online) Cross-plot of Fe_{HR}/Fe_T v. Fe_{Py}/Fe_{HR} for samples with Fe_T >0.5 wt % from the Wangjiaping section. Threshold values of Fe_{HR}/Fe_T (0.38) for oxic-anoxic conditions and Fe_{Py}/Fe_{HR} (0.7-0.8) for ferruginous-euxinic conditions from Poulton & Canfield (2011).

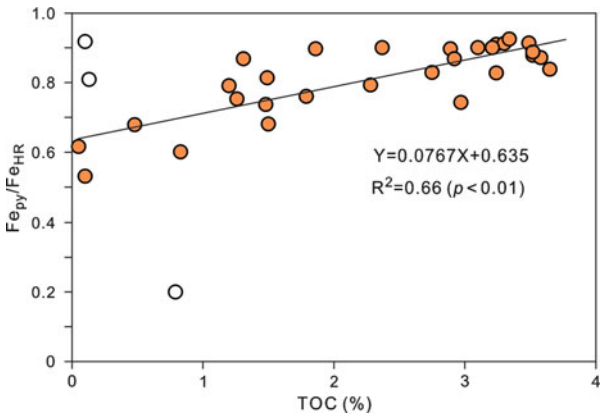

Figure 4. (Colour online) Cross-plot of TOC v. Fe_{Py}/Fe_{HR} for Wangjiaping section. Note that the three samples which are considered as outliers (unfilled symbols) were not included in the correlation.

UM (15–21 m) of the Shuijingtuo Formation. Ti ranges over 0.05–0.53 % (mean 0.33 %) and over 0.03–0.19 % (mean 0.10 %) in the LM and UM, respectively. Fe_U ranges over 0–2.4 % (mean 0.68 %) and over 0.07–0.71 % (mean 0.30 %) in the LM and UM, respectively. Ti and Fe_U exhibit similar patterns of stratigraphic variation to Al: increasing upsection within the LM and then decreasing upsection within the UM.

Fe_T ranges over 1.27–5.18 % (mean 3.40 %), roughly increasing upsection in the LM; it ranges over 0.32–1.8 % (mean 1.09 %), decreasing upsection in the UM. Fe_{HR}/Fe_T ratio over the range 0.47–1.00 (0.82 ± 0.17; mean $\pm 1\sigma$), decreasing upsection in the LM; it varies over 0.60–0.93 (0.78 ± 0.12), increasing upsection in the UM. Fe_{Py}/Fe_{HR} ratios vary over the range 0.03–0.93 (0.77 ± 0.20), and show a generally decreasing trend upsection.

5. Discussion

5.a. Basis for stratigraphic correlation of lower Cambrian deposits in South China

The stratigraphic division and correlation of lower Cambrian units on the Yangtze Block are mainly based on fossils such as small shelly faunas (SSFs) and trilobites (Yuan & Zhao, 1999; Yang *et al*. 2003; Zhu *et al*. 2003; Yang, Zhu & Zhang, 2005; Steiner *et al*. 2007), distinctive marker beds such as a black shale and Ni–Mo layer at the base of the Cambrian (Yang *et al*. 2003; Zhu *et al*. 2003; Jiang *et al*. 2012; Chen *et al*. 2015*a*), and some zircon ages (Wang *et al*. 2012; Chen *et al*. 2015*a*). The presence of SSFA1 and SSFA3 in the lower and upper Yanjiahe Formation suggest the Cambrian Fortunian Age (*c*. 541–529 Ma) and Age 2 (*c*. 529–521 Ma), respectively (Steiner *et al*. 2007; Peng, Babcock & Cooper, 2012). The U–Pb zircon age of 526.4 ± 5.4 Ma from ash beds at the base of

https://doi.org/10.1017/S0016756816001138 Published online by Cambridge University Press

the Shuijingtuo Formation black shale at nearby Wuhe section also indicates a Cambrian Age 2 (Okada *et al*. 2014). The Shuijingtuo Formation contains trilobites such as *S. chanyangensis*, *H. orientalis* and *Metaredlichia* sp., which are of Cambrian Age 3 (*c.* 521–514 Ma), in which the first appearance of *H. orientalis* from the calcareous mudstone and muddy limestone marks the base of *Yunnanaspis–Yiliangella* trilobite Zone in the Hongjingshao Formation from some sections of Yunnan Province (e.g. Xiaotan; Yang, Zhu & Zhang, 2005). We should note that, although the Ni–Mo ore layer is the marker bed for the boundary of Cambrian ages 2 and 3 (*c.* 521 Ma; Zhu *et al*. 2003), it was not found at Wangjiaping. However, this layer was reported at the base of the Shuijingtuo Formation in the nearby Jijiawan (*c.* 10 km to the west) and Yanjiahe (*c.* 30 km to the SW) sections of the Yangtze Gorges region (Chen *et al*. 2015*b*). At Wangjiaping, the Ni–Mo ore layer may be located in an inaccessible covered interval. The framework of stratigraphic correlations mentioned above, which was discussed in greater detail by Jin *et al*. (2016), provides a solid basis for the stratigraphic correlations among the study sections in Figure 5.

5.b. Marine redox conditions at Wangjiaping

Sedimentary iron speciation has been widely used to distinguish oxic, ferruginous and euxinic conditions in siliciclastic rocks as well as in carbonate rocks with >0.5 % Fe_T (e.g. Lyons & Severman, 2006; Canfield *et al*. 2008; Li *et al*. 2010, 2012; Poulton & Canfield, 2011; Clarkson *et al*. 2014). Modern and ancient anoxic sediments yield Fe_{HR}/Fe_T ratios >0.38 through addition of Fe_{HR} from the anoxic water column (Raiswell & Canfield, 1998). Under anoxic and sulphidic (euxinic) conditions, Fe_{HR} tends to be converted to Fe_{py} through its reaction with H_2S to form pyrite, resulting in Fe_{py}/Fe_{HR} ratios of >0.7–0.8 (Poulton & Canfield, 2011).

All samples in the lower Shuijingtuo Formation (0–15 m; i.e. LM) are characterized by >0.5 % Fe_T, elevated Fe_{HR}/Fe_T ratios (>0.38) and high Fe_{py}/Fe_{HR} ratios (0.60–0.93; mean 0.84), suggesting dominantly euxinic conditions punctuated by ferruginous episodes (Figs 2, 3). Samples from the upper Shuijingtuo Formation (15–21 m; i.e. UM) exhibit Fe_T >0.5 % (except for two at 18.12 and 19.15 m), elevated Fe_{HR}/Fe_T ratios (>0.38) and low Fe_{py}/Fe_{HR} ratios (<0.7), indicating ferruginous conditions. Iron speciation data at Wangjiaping therefore suggest a redox transition from dominantly euxinic conditions in the LM to ferruginous conditions in the UM of the Shuijingtuo Formation.

5.c. Interpreting the pyrite sulphur isotope record

The isotopic composition of sulphur in sedimentary pyrite ($\delta^{34}S_{py}$) has been widely used to explore biogeochemical cycling of sulphur in the Earth-surface system (e.g. Scott *et al*. 2014). Among other things, pyrite $\delta^{34}S$ can provide important insights into the influence of seawater sulphate concentrations on the development of mid-depth euxinia (e.g. Feng *et al*. 2014). Variation in $\delta^{34}S_{py}$ depends mainly on the fraction of pyrite burial (f_{py}), the isotopic composition of sulphur entering ocean ($\delta^{34}S_{in}$) and fractionation during microbial sulphate reduction (MSR) (ε_{MSR}). MSR enriches sulphide in the light isotopes of sulphur relative to the seawater sulphate source. Many factors influence ε_{MSR} in nature, including aqueous sulphate concentrations, sulphur oxidation and disproportionation, environments of pyrite formation, and MSR rates (e.g. Canfield & Teske, 1996; Habicht *et al*. 2002; Jones & Fike, 2013; Leavitt *et al*. 2013; Algeo *et al*. 2015). MSR can produce a fractionation of ≥60 ‰ under sulphate-replete conditions (Canfield, Farquhar & Zerkle, 2010; Sim, Bosak & Ono, 2011), whereas sulphate-poor conditions yield minimal fractionation (e.g. <10 ‰ at 200 μM SO_4^{2-}; Habicht *et al*. 2002; Gomes & Hurtgen, 2013; Crowe *et al*. 2014). In addition to MSR, sulphur oxidation and disproportionation can lead to a significant increase in ε_{MSR} (Canfield & Teske, 1996). With other factors held constant, high and low MSR rates result in reduced and increased isotopic fractionation, respectively, yielding values ranging over 0–70 ‰ (Sim, Bosak & Ono, 2011).

Our iron speciation data suggest that the Wangjiaping environment was continuously anoxic throughout the study interval, with samples in the LM and UM of the Shuijingtuo Formation accumulating under dominantly euxinic and ferruginous conditions, respectively (Section 5.b). Sulphur oxidation and disproportionation would therefore have had little to no influence on $\delta^{34}S_{py}$ values in the study section. Given dominantly euxinic conditions in the LM of the Shuijingtuo Formation, pyrite would have formed mainly in the water columns. This unit shows intermediate $\delta^{34}S_{py}$ values at 0–8 m (–10.7 to +3.9 ‰, mean –0.2 ‰), followed by a shift to more negative values at 8–12 m (–14.1 to 6.0 ‰, mean –6.7 ‰; Fig. 2). Relative to early Cambrian seawater sulphate, which had a $\delta^{34}S$ value of +35 to +40 ‰ (Kampschulte & Strauss, 2004; Goldberg, Poulton & Strauss, 2005), these $\delta^{34}S_{py}$ values indicate large MSR fractionations, that is, $\varepsilon_{MSR} \approx$ 29–54 ‰. This range of fractionations yields estimated seawater sulphate concentrations of *c.* 8–30 mM based on the MSR trend method of Algeo *et al*. (2015), that is, close to or somewhat lower than the modern seawater level of 29 mM. The negative shift in $\delta^{34}S_{py}$ values upsection in the LM is roughly correlated with a decrease in organic matter as suggested by TOC, as well as the enhanced riverine flux as suggested by a rise of Al, Ti and Fe_U (Fig. 2), suggesting that the reduced MSR rate caused by a decrease in organic matter loading, or/and a rise of relatively ^{34}S-depleted riverine sulphate to MSR, may have led to the decreasing $\delta^{34}S_{py}$ values. The later mechanism has been proposed to explain the decrease of $\delta^{34}S_{py}$ values from the correlative strata in the inner-shelf Shatan, outer-shelf

https://doi.org/10.1017/S0016756816001138 Published online by Cambridge University Press

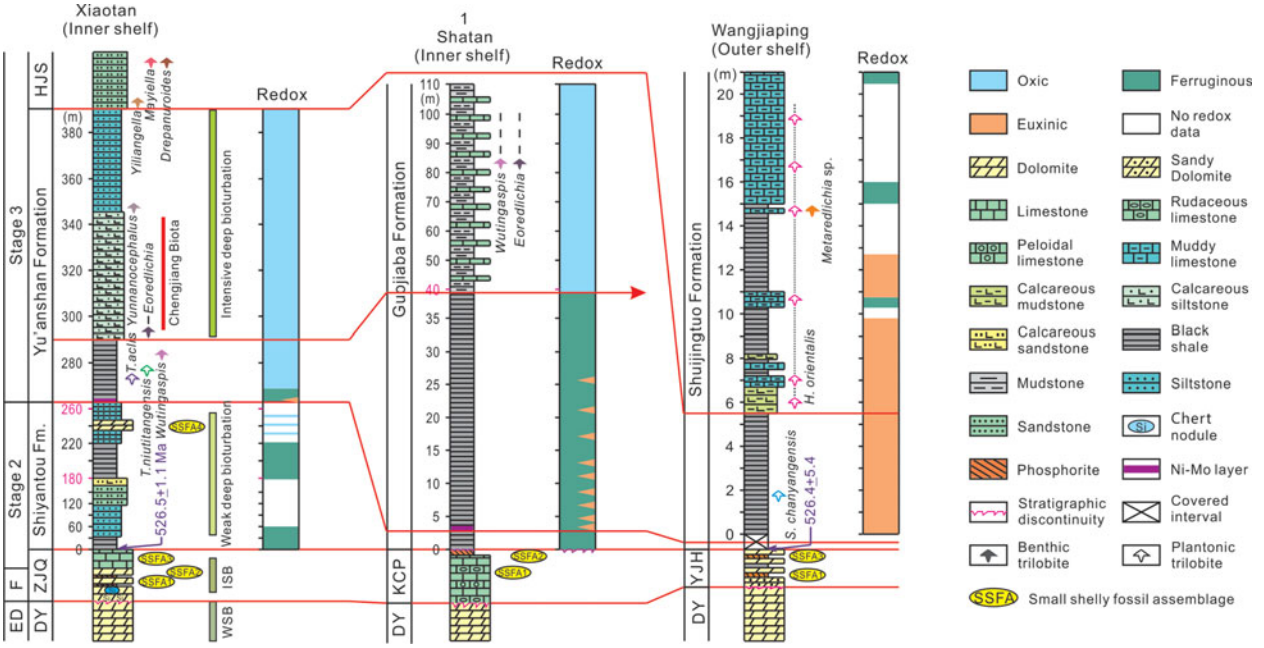

Figure 5. (Colour online) Comparison of fossil records with water-column redox conditions across the Yangtze Block, as reconstructed from geochemical data for Xiaotan, Shatan and Wangjiaping. The U–Pb age at Xiaotan is from the nearby Meichucun section (Compston *et al*. 2008). The lithostratigraphy, biostratigraphy and redox conditions of the Xiaotan and Shatan sections were discussed in detail by Feng *et al*. (2014) and Jin *et al*. (2016), while related data of the Wangjiaping are from this study. See Section 5.a. for the basis of stratigraphic correlation between these sections. Abbreviations: ZJQ – Zhujiaqing Formation; HJS – Hongjingshao Formation; and KCP – Kuanchuanpu Formation.

Yangjiaping and Weng'an sections of the Yangtze Block (Feng *et al*. 2014; Jin *et al*. 2016).

Given ferruginous conditions in the UM of the Shuijingtuo Formation (Section 5.b), the study section was probably located around the chemocline (e.g. in the upper region of the oceanic thermocline), and pyrite formation increasingly occurred in the sediments. Low sulphate concentrations can develop within the sediment when sulphate consumption exceeds supply through diffusion, a condition that limits the degree of sulphur isotopic fractionation expressed between pyrite and porewater sulphate (e.g. Lyons *et al*. 2003). Reduced diffusion of sulphate from the overlying water column into the sediment may therefore have caused the $\delta^{34}S_{py}$ values to shift positively and to fall in a wide range (–4.8 to +19.3 ‰, mean +8.9 ‰) in the UM of the Shuijingtuo Formation (Fig. 2).

5.d. Controls on development of euxinia at Wangjiaping

The tendency of anoxic waters toward euxinic versus ferruginous conditions depends on the relative fluxes of Fe_{HR} and H_2S, with production of the latter controlled mainly by microbial sulphate reduction (MSR) linked to organic matter decay (Raiswell & Canfield, 2012; Feng *et al*. 2014). Given a certain Fe_{HR} supply in a marine system, the spatiotemporal occurrence of euxinia may have been controlled mainly by the local availability of marine organic matter and/or seawater sulphate (Li *et al*. 2010, 2012, 2015*a*).

A large change in $\delta^{34}S_{py}$ values from proximal to distal areas of a marine system is indicative of a gradient in seawater sulphate concentrations. The early Cambrian Yangtze Block exhibits such a gradient, with a mean $\delta^{34}S_{py}$ of –12.0 ‰ in the inner-shelf Xiaotan section, shifting progressively to a mean of +22.5 ‰ in the basinal Longbizui section (Feng *et al*. 2014; Jin *et al*. 2016). Within this interpretative framework, the outer-shelf Wangjiawan section of the present study exhibits intermediate $\delta^{34}S_{py}$ (–2.1 ± 5.3 ‰) and TOC (2.4 ± 1.1 %) values (Fig. 2). These values are nonetheless substantially lower than in the correlative outer-shelf Yangjiaping ($\delta^{34}S_{py}$ = +8.3 ± 4.7 ‰, TOC = 10.7 ± 2.6 %), slope Songtao ($\delta^{34}S_{py}$ = +8.6 ± 7.7 ‰, TOC = 8.3 ± 4.0 %) and slope Longbizui sections ($\delta^{34}S_{py}$ = +21.0 ± 6.8 ‰, TOC = 6.2 ± 1.7 %) (Feng *et al*. 2014). Note that all sections accumulated under euxinic conditions except for Longbizui, where ferruginous conditions prevailed. In view of these relationships, the relative fluxes of sulphate to organic matter at Wangjiaping are inferred to have been higher than in the other, deeper-water sections. When anoxic conditions are indicated in palaeomarine systems, the relative availability of organic matter versus sulphate is therefore likely to play a key role in the development of euxinia.

If our hypothesis is correct, we should expect to see increasing euxinic tendency along with increasing productivity at Wangjiaping instead of at those deeper sites. Indeed, a strong positive correlation between TOC and Fe_{py}/Fe_{HR} (R^2 = 0.66; p < 0.01) was observed for samples (note that all have Fe_T > 0.5 %) at Wangjiaping (Fig. 4). However, only weak correlations between TOC and Fe_{py}/Fe_{HR} (R^2 ≤ 0.22) for anoxic

https://doi.org/10.1017/S0016756816001138 Published online by Cambridge University Press

samples were observed from correlative strata at the outer-shelf Yangjiaping, slope Songtao and Longbizui sections (Feng *et al*. 2014). These observations provide compelling evidence for organic control on the local euxinic formation at Wangjiawan and the high spatial heterogeneity of marine sulphate concentration recently recognized in Neoproterozoic–Cambrian oceans (Li *et al*. 2010, 2012; Feng *et al*. 2014; Jin *et al*. 2014, 2016).

5.e. Spatial variation of early Cambrian redox conditions and metazoan evolution

The early Cambrian evolution of metazoans recorded by fossil distributions is characterized by a highly spatial heterogeneity in South China as well as in the global ocean (e.g. Steiner *et al*. 2007; Zhu, 2010). In Cambrian Fortunian and Stage 2 strata, SSFA1 and SSFA3 were widely found in shelf settings on the Yangtze Block as well as on other cratons (Steiner *et al*. 2007; Peng, Babcock & Cooper, 2012; Landing *et al*. 2013). However, SSFA2 (represented by *Paragloborilus subglobosus – Purella squamulosa*) and SSFA4 (represented by *Sinosachites flabelliformis – Tannuolina zhangwentangi*) are restricted to a few locales on the Yangtze Block (e.g. eastern Yunnan and Sichuan provinces; Steiner *et al*. 2007). In Cambrian Stage 3 deposits, planktonic and benthic trilobites appear in shallow-water sections on the Yangtze Block (e.g. in Yunnan, Sichuan and parts of Guizhou Province; Zhu, 2010), whereas few benthic but abundant planktonic trilobites were found in relatively deeper-water settings (e.g. in the Yangtze Gorges region of Hubei Province and the Weng'an and Songtao sections in Guizhou Province; Xiang *et al*. 1987; Yang *et al*. 2003; Zhu *et al*. 2003). During early Cambrian time, shallow-water settings globally are characterized by more intensive bioturbation than deep-water settings (Buatois *et al*. 2016). A similar pattern exists on the Yangtze Block, as shown by a transition from weak to intensive bioturbation beginning at the base of Cambrian Stage 3 strata in the inner-shelf Xiaotan section, but a complete lack of bioturbation in coeval strata of the outer-shelf Wangjiaping section (Fig. 5; Xiang *et al*. 1987; Shields-Zhou & Zhu, 2013).

Because animals need oxygen to sustain their metabolism, the spatial variability of redox conditions in early Cambrian oceans may have directly controlled the spatial pattern of metazoan distribution. Where euxinic or ferruginous conditions existed, rare benthic fossils are found. The appearance of benthic trilobites such as *Eoredlichia* and *Wutingaspis* coincided with the development of persistently oxic bottom-water conditions, for example, beginning in Cambrian Stage 3 deposits of the inner-shelf Xiaotan and Shatan sections. However, only planktonic trilobites such as *S. changyangensis* and *H. orientalis* are present in correlative strata deposited under euxinic bottom-water conditions in the outer-shelf Wangjiaping section (Fig. 5). Given that benthic trilobites have been found in black shale, mudstone, calcareous siltstone, muddy limestone and sandstone facies (Yang *et al*. 2003; Zhu *et al*. 2003; Zhu, 2010; this study), the spatial distribution of these fossils does not appear to have been controlled by lithology. The fact that euxinic conditions inhibit organic decay and enhance fossil preservation (Gaines *et al*. 2012; Wang *et al*. 2014) suggests that the spatial heterogeneity of fossil distribution on the early Cambrian Yangtze Block does not reflect differential taphonomic effects, because benthic trilobites should have been preserved if they indeed lived in euxinic waters. We therefore infer that spatial variability in marine redox conditions was a key control on metazoan distribution and marine ecosystem development in early Cambrian oceans (cf. Gilleaudeau & Kah, 2015; Li *et al*. 2015*b*).

Variability in patterns of bioturbation in early Cambrian oceans (Buatois *et al*. 2016) may also have been linked to spatial heterogeneity in redox conditions (Jin *et al*. 2016). Reduced benthic oxygen levels have been shown to correlate with shorter burrow lengths and lower burrow densities (Sturdivant, Diaz & Cutter, 2012). In the Yangtze Block, bioturbation occurred in the shallow-water setting (e.g. Xiaotan; Shields-Zhou & Zhu, 2013) with oxic conditions, but no bioturbation was found in the relatively deeper-water settings (e.g. Wangjiaping) with euxinic conditions (Fig. 5). Furthermore, similarly, widespread anoxic conditions during early Cambrian time, possible due to low oxygen levels of less than 40 % present in the atmosphere (Sperling *et al*. 2015), could have resulted in the protracted development of bioturbation (Tarhan *et al*. 2015), whereas the expansion of shelf oxic waters during Cambrian Age 3 (Jin *et al*. 2016) might be responsible for the increase in bioturbation (Buatois *et al*. 2016).

6. Conclusions

This study presents Fe-C-S-Al-Ti geochemical data from lower Cambrian strata of the outer-shelf Wangjiaping section on the Yangtze Block of South China. Iron speciation data indicate a redox change from dominantly euxinic to ferruginous conditions during Cambrian Age 3, accompanied by a fall in sea level. A good correlation between TOC and Fe_{py}/Fe_{HR} suggests that organic matter availability limited development of euxinia at Wangjiaping. Pyrite $\delta^{34}S$ is more negative than that in correlative deeper-water sections, suggesting higher sulphate concentrations at Wangjiaping. These observations are consistent with the hypothesis that the relative availability of sulphate versus organic matter controlled development of euxinia in the lower Cambrian strata of South China, and that organic matter was relatively limiting at Wangjiaping whereas sulphate was relatively limiting in deeper-water sections. Our work therefore provides evidence for the marine sulphate gradients from proximal to distal oceans previously proposed for Neoproterozoic–Cambrian oceans.

https://doi.org/10.1017/S0016756816001138 Published online by Cambridge University Press

Redox conditions in comparison with fossils in shelf sections, including inner-shelf Xiaotan and Shatan and outer-shelf Wangjiaping, show that planktonic and benthic trilobites lived in oxic conditions, whereas only planktonic trilobites thrived in water masses having anoxic or euxinic bottom-water conditions. Further correlation suggests that bioturbation occurred in conjunction with oxic conditions, whereas no bioturbation developed under anoxic to euxinic bottom-water conditions. Similar patterns of spatial heterogeneities are inferred to have existed for redox conditions and animal evolution globally. These findings therefore suggest that the spatial heterogeneity of redox conditions in the shelf settings may have played a key role in the spatial distribution of early animals during early Cambrian time.

Acknowledgements. We thank Shida Tang and Haiyang Wang for laboratory assistance. This study was supported by the Chinese 973 program (grant no. 2013CB955704) and the NSFC (grant no. 41172030). Research by TJA is supported by the US National Science Foundation (Sedimentary Geology and Paleobiology program, grant no. EAR-1053449), the NASA Exobiology program (grant no. NNX13AJ1IG) and the China University of Geosciences-Wuhan (SKL-GPMR program GPMR201301 and SKL-BGEG program BGL21407).

References

Algeo, T. J., Luo, G. M., Song, H. Y., Lyons, T. W. & Canfield, D. E. 2015. Reconstruction of secular variation in seawater sulfate concentrations. *Biogeosciences* **12**(7), 2131–51.

Buatois, L. A., Mángano, M. G., Olea, R. A. & Wilson, M. A. 2016. Decoupled evolution of soft and hard substrate communities during the Cambrian Explosion and Great Ordovician Biodiversification Event. *Proceedings of the National Academy of Sciences of the United States of America* **113**(25), 6945–8.

Butterfield, N. J. 2007. Macroevolution and macroecology through deep time. *Palaeontology* **50**(1), 41–55.

Butterfield, N. J. 2011. Animals and the invention of the Phanerozoic Earth system. *Trends in Ecology & Evolution* **26**(2), 81–7.

Canfield, D. E., Farquhar, J. & Zerkle, A. L. 2010. High isotope fractionations during sulfate reduction in a low-sulfate euxinic ocean analog. *Geology* **38**(5), 415–18.

Canfield, D. E., Poulton, S. W., Knoll, A. H., Narbonne, G. M., Ross, G., Goldberg, T. & Strauss, H. 2008. Ferruginous conditions dominated later Neoproterozoic deep-water chemistry. *Science* **321**(5891), 949–52.

Canfield, D. E., Raiswell, R., Westrich, J. T., Reaves, C. M. & Berner, R. A. 1986. The use of chromium reduction in the analysis of reduced inorganic sulfur in sediments and shales. *Chemical Geology* **54**(1–2), 149–55.

Canfield, D. E. & Teske, A. 1996. Late Proterozoic rise in atmospheric oxygen concentration inferred from phylogenetic and sulphur-isotope studies. *Nature* **382**(6587), 127–32.

Chen, D., Zhou, X., Fu, Y., Wang, J. & Yan, D. 2015*a*. New U-Pb zircon ages of the Ediacaran-Cambrian boundary strata in South China. *Terra Nova* **27**(1), 62–68.

Chen, P. 1984. Discovery of Lower Cambrian small shelly fossils from Jijiapo, Yichang, west Hubei and its significance. *Professional Papers of Stratigraphy and Palaeontology* **13**, 49–66 (in Chinese with English abstract).

Chen, X., Ling, H. F., Vance, D., Shields-Zhou, G. A., Zhu, M., Poulton, S. W., Och, L. M., Jiang, S. Y., Li, D., Cremonese, L. & Archer, C. 2015*b*. Rise to modern levels of ocean oxygenation coincided with the Cambrian radiation of animals. *Nature Communications* **6**, 7142.

Clarkson, M., Poulton, S., Guilbaud, R. & Wood, R. 2014. Assessing the utility of Fe/Al and Fe-speciation to record water column redox conditions in carbonate-rich sediments. *Chemical Geology* **382**, 111–22.

Compston, W., Zhang, Z., Cooper, J. A., Ma, G. & Jenkins, R. J. F. 2008. Further SHRIMP geochronology on the early Cambrian of South China. *American Journal of Science* **308**(4), 399–420.

Crowe, S. A., Paris, G., Katsev, S., Jones, C., Kim, S. T., Zerkle, A. L., Nomosatryo, S., Fowle, D. A., Adkins, J. F., Sessions, A. L., Farquhar, J. & Canfield, D. E. 2014. Sulfate was a trace constituent of Archean seawater. *Science* **346**(6210), 735–9.

Feng, L., Li, C., Huang, J., Chang, H. & Chu, X. 2014. A sulfate control on marine mid-depth euxinia on the early Cambrian (ca. 529–521 Ma) Yangtze platform, South China. *Precambrian Research* **246**, 123–33.

Gaines, R. R., Hammarlund, E. U., Hou, X. G., Qi, C. S., Gabbott, S. E., Zhao, Y. L., Peng, J. & Canfield, D. E. 2012. Mechanism for Burgess Shale-type preservation. *Proceedings of the National Academy of Sciences of the United States of America* **109**(14), 5180–4.

Gilleaudeau, G. J. & Kah, L. C. 2015. Heterogeneous redox conditions and a shallow chemocline in the Mesoproterozoic ocean: Evidence from carbon–sulfur–iron relationships. *Precambrian Research* **257**, 94–108.

Goldberg, T., Poulton, S. W. & Strauss, H. 2005. Sulphur and oxygen isotope signatures of late Neoproterozoic to early Cambrian sulphate, Yangtze Platform, China: diagenetic constraints and seawater evolution. *Precambrian Research* **137**(3), 223–41.

Goldberg, T., Strauss, H., Guo, Q. & Liu, C. 2007. Reconstructing marine redox conditions for the Early Cambrian Yangtze Platform: evidence from biogenic sulphur and organic carbon isotopes. *Palaeogeography, Palaeoclimatology, Palaeoecology* **254**(1), 175–93.

Gomes, M. L. & Hurtgen, M. T. 2013. Sulfur isotope systematics of a euxinic, low-sulfate lake: Evaluating the importance of the reservoir effect in modern and ancient oceans. *Geology* **41**(6), 663–6.

Habicht, K. S., Gade, M., Thamdrup, B., Berg, P. & Canfield, D. E. 2002. Calibration of sulfate levels in the Archean ocean. *Science* **298**(5602), 2372–4.

Jiang, G., Wang, X., Shi, X., Xiao, S., Zhang, S. & Dong, J. 2012. The origin of decoupled carbonate and organic carbon isotope signatures in the early Cambrian (ca. 542–520 Ma) Yangtze platform. *Earth and Planetary Science Letters* **317–8**, 96–110.

Jin, C., Li, C., Algeo, T. J., Planavsky, N. J., Cui, H., Yang, X., Zhao, Y., Zhang, X. & Xie, S. 2016. A highly redox-heterogeneous ocean in South China during the early Cambrian (~529–514 Ma): Implications for biota-environment co-evolution. *Earth and Planetary Science Letters* **441**, 38–51.

Jin, C., Li, C., Peng, X., Cui, H., Shi, W., Zhang, Z., Luo, G. & Xie, S. 2014. Spatiotemporal variability of ocean

chemistry in the early Cambrian, South China. *Science China Earth Sciences* **57**(4), 579–91.

Jones, D. S. & Fike, D. A. 2013. Dynamic sulfur and carbon cycling through the end-Ordovician extinction revealed by paired sulfate–pyrite δ^{34}S. *Earth and Planetary Science Letters* **363**, 144–55.

Kampschulte, A. & Strauss, H. 2004. The sulfur isotopic evolution of Phanerozoic seawater based on the analysis of structurally substituted sulfate in carbonates. *Chemical Geology* **204**(3–4), 255–86.

Knoll, A. H. & Carroll, S. B. 1999. Early animal evolution: emerging views from comparative biology and geology. *Science* **284**(5423), 2129–37.

Landing, E., Geyer, G., Brasier, M. D. & Bowring, S. A. 2013. Cambrian Evolutionary Radiation: Context, correlation, and chronostratigraphy—Overcoming deficiencies of the first appearance datum (FAD) concept. *Earth-Science Reviews* **123**, 133–72.

Leavitt, W. D., Halevy, I., Bradley, A. S. & Johnston, D. T. 2013. Influence of sulfate reduction rates on the Phanerozoic sulfur isotope record. *Proceedings of the National Academy of Sciences of the United States of America* **110**(28), 11244–9.

Li, C., Cheng, M., Algeo, T. J. & Xie, S. 2015*a*. A theoretical prediction of chemical zonation in early oceans (>520 Ma). *Science China Earth Sciences* **58**(11), 1901–09.

Li, C., Love, G. D., Lyons, T. W., Fike, D. A., Sessions, A. L. & Chu, X. 2010. A stratified redox model for the Ediacaran ocean. *Science* **328**(5974), 80–3.

Li, C., Love, G. D., Lyons, T. W., Scott, C. T., Feng, L., Huang, J., Chang, H., Zhang, Q. & Chu, X. 2012. Evidence for a redox stratified Cryogenian marine basin, Datangpo Formation, South China. *Earth and Planetary Science Letters* **331**, 246–56.

Li, C., Planavsky, N. J., Shi, W., Zhang, Z., Zhou, C., Cheng, M., Tarhan, L. G., Luo, G. & Xie, S. 2015*b*. Ediacaran marine redox heterogeneity and early animal ecosystems. *Scientific Reports* **5**, article number: 17097, doi:10.1038/srep17097.

Li, C., Zhu, M. & Chu, X. 2016. Atmospheric and oceanic oxygenation and evolution of early life on Earth: New contributions from China. *Journal of Earth Science* **27**(2), 167–9.

Lyons, T. W. & Severmann, S. 2006. A critical look at iron paleoredox proxies: New insights from modern euxinic marine basins. *Geochimica et Cosmochimica Acta* **70**(23), 5698–722.

Lyons, T. W., Werne, J. P., Hollander, D. J. & Murray, R. W. 2003. Contrasting sulfur geochemistry and Fe/Al and Mo/Al ratios across the last oxic-to-anoxic transition in the Cariaco Basin, Venezuela. *Chemical Geology* **195**(1–4), 131–57.

Nursall, J. 1959. Oxygen as a prerequisite to the origin of the Metazoa. *Nature* **183**, 1170–72.

Och, L. M., Cremonese, L., Shields-Zhou, G. A., Poulton, S. W., Struck, U., Ling, H., Li, D., Chen, X., Manning, C. & Thirlwall, M. 2016. Palaeoceanographic controls on spatial redox distribution over the Yangtze Platform during the Ediacaran-Cambrian transition. *Sedimentology* **63**, 378–410.

Okada, Y., Sawaki, Y., Komiya, T., Hirata, T., Takahata, N., Sano, Y., Han, J. & Maruyama, S. 2014. New chronological constraints for Cryogenian to Cambrian rocks in the Three Gorges, Weng'an and Chengjiang areas, South China. *Gondwana Research* **25**(3), 1027–44.

Peng, S., Babcock, L. & Cooper, R. 2012. *The Cambrian Period*. In *The Geologic Time Scale*, 1st edition (eds F. M. Gradstein, J.G. Ogg, M. Schmitz & G. Ogg), pp. 437–88. Amsterdam, Boston: Elsevier B.V.

Poulton, S. W. & Canfield, D. E. 2005. Development of a sequential extraction procedure for iron: implications for iron partitioning in continentally derived particulates. *Chemical Geology* **214**(3), 209–21.

Poulton, S. W. & Canfield, D. E. 2011. Ferruginous conditions: a dominant feature of the ocean through Earth's history. *Elements* **7**(2), 107–12.

Raiswell, R. & Canfield, D. E. 1998. Sources of iron for pyrite formation in marine sediments. *American Journal of Science* **298**(3), 219–45.

Raiswell, R. & Canfield, D. E. 2012. The iron biogeochemical cycle past and present. *Geochemical Perspectives* **1**(1), 1–220.

Scott, C., Wing, B. A., Bekker, A., Planavsky, N. J., Medvedev, P., Bates, S. M., Yun, M. & Lyons, T. W. 2014. Pyrite multiple-sulfur isotope evidence for rapid expansion and contraction of the early Paleoproterozoic seawater sulfate reservoir. *Earth and Planetary Science Letters* **389**, 95–104.

Shields-Zhou, G. & Zhu, M. 2013. Biogeochemical changes across the Ediacaran–Cambrian transition in South China. *Precambrian Research* **225**, 1–6.

Shu, D., Isozaki, Y., Zhang, X., Han, J. & Maruyama, S. 2014. Birth and early evolution of metazoans. *Gondwana Research* **25**(3), 884–95.

Sim, M. S., Bosak, T. & Ono, S. 2011. Large sulfur isotope fractionation does not require disproportionation. *Science* **333**(6038), 74–7.

Sperling, E. A., Frieder, C. A., Raman, A. V., Girguis, P. R., Levin, L. A. & Knoll, A. H. 2013. Oxygen, ecology, and the Cambrian radiation of animals. *Proceedings of the National Academy of Sciences of the United States of America* **110**(33), 13446–51.

Sperling, E. A., Wolock, C. J., Morgan, A. S., Gill, B. C., Kunzmann, M., Halverson, G. P., Macdonald, F. A., Knoll, A. H. & Johnston, D. T. 2015. Statistical analysis of iron geochemical data suggests limited late Proterozoic oxygenation. *Nature* **523**(7561), 451–4.

Steiner, M., Li, G., Qian, Y., Zhu, M. & Erdtmann, B.-D. 2007. Neoproterozoic to Early Cambrian small shelly fossil assemblages and a revised biostratigraphic correlation of the Yangtze Platform (China). *Palaeogeography, Palaeoclimatology, Palaeoecology* **254**(1–2), 67–99.

Sturdivant, S. K., Diaz, R. J. & Cutter, G. R. 2012. Bioturbation in a declining oxygen environment, in situ observations from Wormcam. *Plos One* **7**(4), doi: 10.1371/journal.pone.0034539.

Tarhan, L. G., Droser, M. L., Planavsky, N. J. & Johnston, D. T. 2015. Protracted development of bioturbation through the early Palaeozoic Era. *Nature Geoscience* **8**, 865–9.

Wang, J. & Li, Z.-X. 2003. History of Neoproterozoic rift basins in South China: implications for Rodinia breakup. *Precambrian Research* **122**, 141–58.

Wang, W., Guan, C., Zhou, C., Wan, B., Tang, Q., Chen, X., Chen, Z. & Yuan, X. 2014. Exceptional preservation of macrofossils from the Ediacaran Lantian and Miaohe Biotas, South China. *Palaios* **29**(3), 129–36.

Wang, X., Shi, X., Jiang, G. & Zhang, W. 2012. New U–Pb age from the basal Niutitang Formation in South China: Implications for diachronous development and condensation of stratigraphic units across the Yangtze platform at the Ediacaran–Cambrian transition. *Journal of Asian Earth Sciences* **48**, 1–8.

Wille, M., Nagler, T. F., Lehmann, B., Schroder, S. & Kramers, J. D. 2008. Hydrogen sulphide release to surface waters at the Precambrian/Cambrian boundary. *Nature* **453**(7196), 767–9.

Xiang, W. L., Zhou, T. M., Ni, S. Z., Zeng, Q. L., Xu, G. H., Lai, C. G., Wang, X. F. & Li, Z. H. 1987. *Cambrian System*. In *Biostratigraphy of the Yangtze Gorge area (2): Early Palaeozoic Era* (eds X. F. Wang, W. L. Xiang, S. Z. Ni, Q. L. Zeng, G. H. Xu, T. M. Zhou, C. G. Lai & Z. H. Li), pp. 4–42. Beijing: Geological Publishing House.

Yang, A., Zhu, M. & Zhang, J. 2005. Stratigraphic distribution and palaeogeographic control on the Early Cambrian eodiscoids in Yangtze Platform. *Journal of Palaeogeography* **7**, 219–232 (in Chinese with English abstract).

Yang, A., Zhu, M., Zhang, J. & Li, G. 2003. Early Cambrian eodiscoid trilobites of the Yangtze Platform and their stratigraphic implications. *Progress in Natural Science* **13**(11), 861–66.

Yang, B., Steiner, M. & Keupp, H. 2015. Early Cambrian palaeobiogeography of the Zhenba–Fangxian Block (South China): Independent terrane or part of the Yangtze Platform? *Gondwana Research* **28**(4), 1543–65.

Yuan, J. L. & Zhao, Y. L. 1999. Subdivision and correlation of Lower Cambrian in southwest China, with a discussion of the age of Early Cambrian series biota. *Acta Palaeontologica Sinica* **38**(Suppl.), 116–31 (in Chinese with English abstract).

Zhang, S., Li, H., Jiang, G., Evans, D. A. D., Dong, J., Wu, H., Yang, T., Liu, P. & Xiao, Q. 2015. New paleomagnetic results from the Ediacaran Doushantuo Formation in South China and their paleogeographic implications. *Precambrian Research* **259**, 130–42.

Zhu, M. 2010. The origin and Cambrian explosion of animals: fossil evidence from China. *Acta Palaeontologica Sinica* **49**, 269–87 (in Chinese with English abstract).

Zhu, M., Zhang, J. & Yang, A. 2007. Integrated Ediacaran (Sinian) chronostratigraphy of South China. *Palaeogeography, Palaeoclimatology, Palaeoecology* **254**(1–2), 7–61.

Zhu, M., Zhang, J., Yang, A., Li, G., Steiner, M. & Erdtmann, B. D. 2003. Sinian-Cambrian stratigraphic framework for shallow- to deep-water environments of the Yangtze Platform: an integrated approach. *Progress in Natural Science* **13**(12), 951–60.